Available online at www.sciencedirect.com
ScienceDirect
JOURNAL OF RARE EARTHS, Vol. 32, No. 11, Nov. 2014, P. 1016
JOURNAL OF RARE EARTHS
www.re-journal.com/en/

Structural studies of $BaTiO_3:Er^{3+}$ and $BaTiO_3:Yb^{3+}$ powders synthesized by hydrothermal method

Garrido-Hernández A[1], García-Murillo A[2,*], Carrillo-Romo F de J[2], Cruz-Santiago L A[3], Chadeyron G[4], Morales-Ramírez A de J[2], Velumani S[5]

(1. T.A. Post-graduate Student. Instituto Politécnico Nacional, CIITEC IPN, Cerrada de Cecati S/N. Col. Santa Catarina, Azcapotzalco México D.F. C.P. 02250, México D.F, México; 2. Instituto Politécnico Nacional, CIITEC IPN, Cerrada de Cecati S/N. Col. Santa Catarina, Azcapotzalco México D.F. C.P. 02250, México D.F; 3. Departament of Engineering Materials, Tecnológico de Estudios Superiores de Coacalco (TESCo), Av. 16 de Septiembre # 54, Cabecera Municipal, C.P. 55700, Coacalco de Berriozábal, Estado de México; 4. Institut de Chimie de Clermont-Ferrand, UMR 6296 CNRS / UBP / ENSCCF 24, avenue des Landais, BP 80026, 63171 Aubière Cedex – France; 5. Department of Electrical Engineering (SEES), Centro de Investigación y de Estudios Avanzados del IPN, Av. Instituto Politécnico Nacional, 2508 Col. San Pedro Zacatenco, C.P. 07360 Mexico, D.F., Mexico)

Received 9 November 2013; revised 28 May 2014

Abstract: Erbium and ytterbium doped barium titanate nanopowders were prepared using the hydrothermal method. A barium titanate structure doped with rare earth ions manifested new characteristics and improved the field of application of optical devices such as trichromatic tubes, LCD displays, lamps, and infrared lasers. In this work, $BaTiO_3:Er^{3+}$ and $BaTiO_3:Yb^{3+}$ were prepared using barium chloride [$BaCl_2$], titanium butoxide [$C_{16}H_{36}O_4Ti$], erbium chloride [$ErCl_3$] and ytterbium chloride [$YbCl_3$] as precursors. Anhydrous methanol was employed as a solvent. Metallic potassium was used to promote solubility in the system and increase the pH to 13. This method yielded the formation of a predominantly cubic structure in both Er^{3+} and Yb^{3+} doped $BaTiO_3$ powders. Characteristic bondings of $BaTiO_3$ were observed with FT-IR spectroscopy. The predominantly cubic structure was confirmed by X-ray diffraction and micro-Raman analyses. The particle size (~30 nm) was estimated using the Scherrer equation and X-ray diffraction data. The results were presented and discussed.

Keywords: nanopowders; hydrothermal; $BaTiO_3:Er^{3+}$; $BaTiO_3:Yb^{3+}$; rare earths

$BaTiO_3$ is a ceramic material with ferroelectric, dielectric and piezoelectric properties. Barium titanate has been thoroughly studied due to specific characteristics (dielectric tunability, high dielectric constant and piezoelectricity[1,2]) that enable it to be widely applied in the electronics industry, such as in multilayer ceramic capacitors, piezoelectric transducers, wireless communication, pyroelectric elements and positive temperature coefficient (PTC) sensors, microphones and opto-electronic devices. The structure of $BaTiO_3$ structure is important because its properties depend on its crystallographic phase. For example, the cubic phase has paraelectric properties, while the tetragonal phase does not exhibit these properties. The barium titanate structure acquired optic properties after doping with rare earths[3,4]. A luminescent effect is provoked by the dopant ion insertion into the $BaTiO_3$ structure; thus, the different emissions observed in the electromagnetic spectrum depend on the characteristics ion dopant. Therefore, barium titanate nanopowders doped with rare earth ions could be used in imaging devices (LCD displays, trichromatic tubes) and optoelectronic devices[5]. Furthermore, promising up-conversion properties of barium titanate nanopowders doped with Er[6], Er-Yb[7] or Yb-Er-Tm[8] were presented[8]. However, the final properties of $BaTiO_3$ depend on the characteristics of the particles. The method of synthesis of barium titanate is very important for controlling the shape, size, ion particle distribution, and crystallographic structure[9,10].

Barium titanate powders have been prepared by different methods; micron-size $BaTiO_3$ powder is generally prepared by solid-state reaction[11], using high temperature ranges (1000–1300 °C); $BaTiO_3$ nanopowders can be synthesized by chemical methods such as the co-precipitation method[12], sol-gel process[13,14], and the hydrothermal method[15,16]. With chemical methods, the nanopowders obtained present a cubic[17] or tetragonal[18] structure. $BaTiO_3$ powders, albeit with large-grained particles with uncontrolled and irregular morphology, were obtained by the microwave sintering method.

Investigations into the size of $BaTiO_3$ particles are of great interest in relation on their dielectric and ferroelectric properties. When the hydrothermal method is used for the sintering of $BaTiO_3$ nanopowders, a small particle

Foundation item: Project supported by CONACYT Through Project 100764 and the IPN Through Projects SIP-2013664, SIP-2013665 and SEP-CONACYT ANUIES PROJECT M09P01

* **Corresponding author:** García-Murillo A (**E-mail:** angarciam@ipn.mx; **Tel.:** +1 52 572960000-68315)

DOI: 10.1016/S1002-0721(14)60176-9

size can be obtained[19]. When the particle size of $BaTiO_3$ is sufficiently small, the paraelectric-ferroelectric phase transition vanishes, and the cubic phase can be stabilized at room temperature, in contrast to the ferroelectric tetragonal form. Recent studies have shown the possibility of stabilizing the cubic phase to yield particles under 30 nm[20,21].

Some researchers have offered hypotheses to explain the effects of grain size on ceramics, which describe the presence of electric fields of depolarization in the compound and tensions in the grain. Arlt et al.[22] suggest that the effect of grain size on the ferroelectric-paraelectric temperature transition is due to tensions present in the grains.

In the present work, structural studies of $BaTiO_3:Er^{3+}$ and $BaTiO_3:Yb^{3+}$ nanopowders synthesized by hydrothermal method were discussed. The samples were characterized by X-ray diffraction (XRD), FTIR and Raman spectroscopies as well as high resolution transmission electron microscopies (HRTEM).

1 Material and methods

Erbium and ytterbium doped $BaTiO_3$ nanopowders were synthesized by the hydrothermal method, using barium chloride [$BaCl_2$], titanium butoxide [$C_{16}H_{36}O_4Ti$], erbium chloride [$ErCl_3$] and ytterbium chloride [$YbCl_3$] as precursors. Anhydrous methanol was used as a solvent. Metallic potassium promoted the solubility in the system and increased the pH to 13. This hydrothermal method allows the formation of a predominantly cubic structure in both Er^{3+}- and Yb^{3+}-doped $BaTiO_3$ powders. For this method, a stainless autoclave of 45 mL was used; the hydrothermal process took place inside the autoclave due to temperature and pressure conditions. The temperature and time were varied during the synthesis of nanoparticles. In order to perform the synthesis, 0.35 g of barium chloride were added to 13 mL of anhydride methanol; while in another container, the ytterbium was dissolved in 2 mL of anhydride methanol. The potassium was dissolved in a controlled atmosphere to avoid the humidity. Finally, to obtain the final dissolution, the above mixtures were combined. The molar ratio used was Ba/Ti= 1.6, to promote barium vacancy. After the synthesis of barium titanate, the obtained powders of barium titanate were cleaned to remove impurities, and after washing, the powders were dried at 90 °C.

The IR spectra were recorded using a Perkin Elmer 2000 FT-IR; the range was 2500–400 cm^{-1}. Raman spectroscopy analysis was conducted with Horiba-Jobin Yvon equipment and a LabRAM HR800 model with 1 cm^{-1} resolution; the studied range was 150–1000 cm^{-1}. The crystallographic phase of $BaTiO_3$ was identified using a diffractometer Bruker AXS D8 Advance; the scan was 0.05 (°)/s, and the 2θ range was 0° to 90°. The $BaTiO_3$ micrographs of the obtained powders were obtained by HRTEM (JEM-2299FS), operating at 200 kV.

2 Results and discussion

2.1 Infrared spectroscopy

The infrared spectra presented in Fig. 1 show absorption peaks at ~1630 cm^{-1}, corresponding to the bending vibrations of O–H corresponding to coordinated H_2O, as well as Ti–OH.

The presence of OH^- groups was originated by hydrolysis of the nanoparticles surface with alcohol and water compounds. The synthesis performed at 180 °C and 36 h produced high quality powders. Fig. 1 shows the fingerprint absorption bands relating to $BaTiO_3$, situated at ~545 and ~410 cm^{-1} [23,24]. The absorption bands correspond to $Ti–O_I$ stretching vibrations and $O_I–Ti–O_{II}$ torsion vibrations, related to the $Ti–O_6$ octahedron[25]. From the synthesis conditions used, it can be observed that the CO_3^{2-} group is characterized by absorption bands in the region 1080–1250 cm^{-1}. $BaCO_3$ compound present in the crystallite was probably due to the reaction of residual Ba^{2+} with CO_2 in the air, mixed into the crystallite after thermal treatment[26]. The $BaTiO_3$ matrix is composed of $Ti–O_6$ octahedrons, and the Ba^{2+} is located at the center of eight $Ti–O_6$ octahedrons. The so-called OH defect is formed by one proton with an oxygen molecule of the octahedron[27]. It requires a charge compensator to maintain the neutrality of the crystallites. The negatively charged cation vacancy could act as the compensator. The $Ti–O_6$ octahedron is the most stable form of Ti^{4+} and is the basic structural element in perovskite $BaTiO_3$. Thus, the Ba^{2+} vacancy is proposed as the most probable compensator.

2.2 XRD analysis

The X-ray diffraction patterns of $BaTiO_3:Er^{3+}$ and $BaTiO_3:Yb^{3+}$ nanopowders are presented in Fig. 2. The pat-

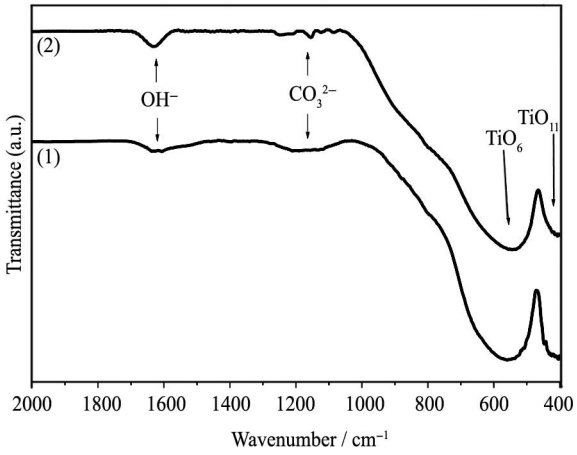

Fig. 1 IR spectra of $BaTiO_3:Er^{3+}$ (5 mol.%) (1) and $BaTiO_3:Yb^{3+}$ (6 mol.%) (2) nanopowders obtained by hydrothermal method

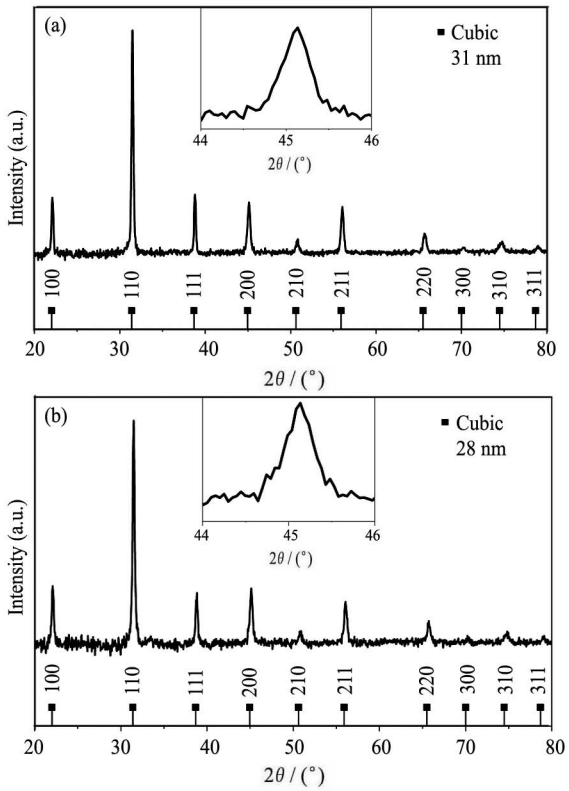

Fig. 2 X-Ray diffraction patterns of $BaTiO_3:Er^{3+}$ (5 mol.%) (a) and $BaTiO_3:Yb^{3+}$ (6 mol.%) (b) nanopowders obtained by hydrothermal method at 180 °C and 36 h

terns were compared with the reference standard of cubic $BaTiO_3$. In addition, the average size of the crystallites was estimated from the broadening of the diffraction peaks, using the Scherrer equation. The estimated sizes were ~30 nm. The presence of the large crystallites randomly dispersed could explain the difference in size in comparison with lower diameter (5 to 10 nm) observed by HRTEM studies.

At first sight, it could be thought that the patterns fit well with the peak position of the standard $BaTiO_3$ cubic phase (JCPDS 792263), since the splitting of the cubic peak at 2θ=45.235° into tetragonal peaks 002 at 2θ= 44.853° and 200 at 2θ=44° (JCPDS 050626) was not observed. However, diffraction peaks were observed at positions corresponding to the meta-stable cubic phase. Such stabilization is known to be common in hydrothermally synthesized $BaTiO_3$ powders, and this is explained by the entrapment of hydroxyl groups in the perovskite lattice.

2.3 Raman spectroscopy

Fig. 3 shows the Raman spectra of the $BaTiO_3:Er^{3+}$ and $BaTiO_3:Yb^{3+}$ nanopowders. Raman spectroscopy is a highly sensitive spectroscopic technique used to probe the local structure of atoms in materials. Based on crystallography, only infrared active bands without first-order Raman activity are predicted for cubic $BaTiO_3$, whereas eight Raman active modes, seven of which are also IR

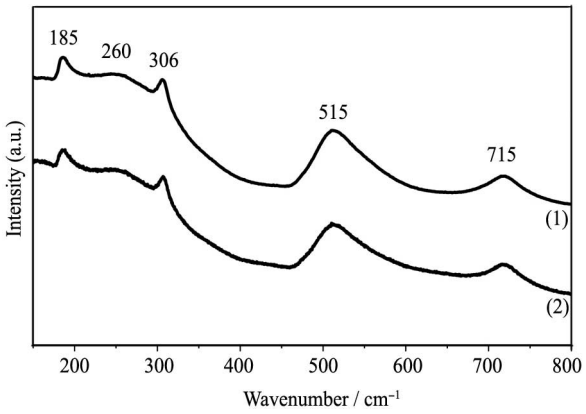

Fig. 3 Raman spectra of $BaTiO_3:Er^{3+}$ (5 mol.%) (1) and $BaTiO_3:Yb^{3+}$ (6 mol.%) (2) nanopowders obtained by hydrothermal method at 180 °C and 36 h

active, are expected for tetragonal $BaTiO_3$ [28].

The tetragonal-cubic transition occurs on the Curie point (130 °C)[29], it can be modified by the small particle sizes (~30 nm)[20,30]. The spectra consist of characteristic bands ascribed to the $BaTiO_3$ phases, at 185, 260, 306, 515 and 715 cm^{-1}.

Peaks appearing at 185, 260, and 515 cm^{-1} were ascribed to the cubic phase of the $BaTiO_3$[31,32], while bands appearing at 306 and 715 cm^{-1}, according to the literature[33], are related to the tetragonal structure. Broadband displacement of 260 cm^{-1} could be related to the particle size and the distorted $BaTiO_3$ lattice[34], provoked by the incorporation of the dopant ion. The results point to the coexistence of the cubic and tetragonal phases, which is recognized by Cifti et al.[35] to exist in the predominantly cubic phase. The splitting peak situated at 2θ~45° is observed only if the tetragonal phase content is higher than 23% in the cubic-tetragonal mixed phases.

2.4 High-resolution transmission electron microscopy (HRTEM)

With the aim of studying the surface structure of $BaTiO_3$ nanocrystals at the atomic scale, HRTEM investigations were carried out. Fig. 4(a, b) and Fig. 5(a, b) show the HRTEM images of the $BaTiO_3:Er^{3+}$ and $BaTiO_3:Yb^{3+}$ nanopowders. TEM observations show the presence of erbium and ytterbium doped barium titanate nanoparticles homogeneously dispersed (Fig. 4(a) and Fig. 5(a), respectively).

Figs. 4(a) and 5(a), which show HRTEM images of the $BaTiO_3$ nanopowders, confirm the presence of $BaTiO_3$ systems characterized by crystallites with sizes from 5 to10 nm.

It is known that in the perovskite structure, the {100} planes have the lowest surface energy, and in turn, they have the lowest planar growth rate[36]. Thus, the equilibrium shape is cubic, as observed in other perovskites (e.g., $PbTiO_3$[37]). In addition, the strain associated with the stabilization of the cubic structure tends to reduce the sur-

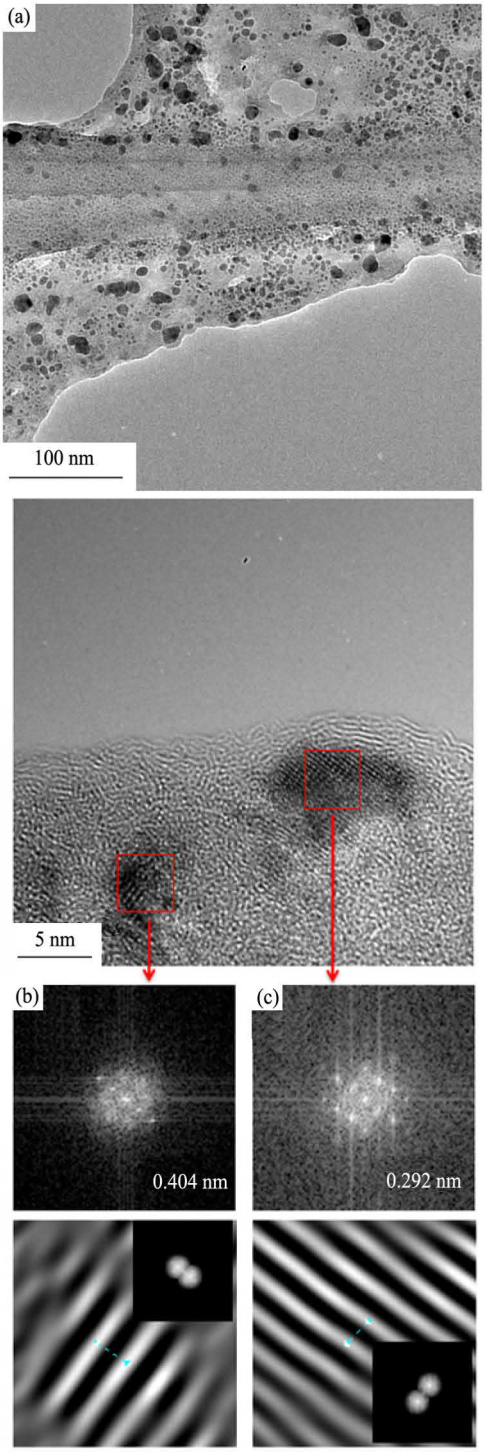

Fig. 4 High-resolution electron micrographs of $BaTiO_3:Er^{3+}$ (5 mol.%) nanopowders obtained by hydrothermal method at 180 °C and 36 h (a, b) and Fourier transforms of the (100) (c) and (110) (d) planes

face area of the growing particles. Therefore, the intermediate morphology consists of cubic particles with a semi-spherical shape, which was regained during the final stage of growth, although some larger particles still retain their cubic shape[38]. The small particle size does not allow for the tetragonal-cubic transition.

HRTEM images show a contrast variation. In a TEM image, large strains are indicated by variations in contrast

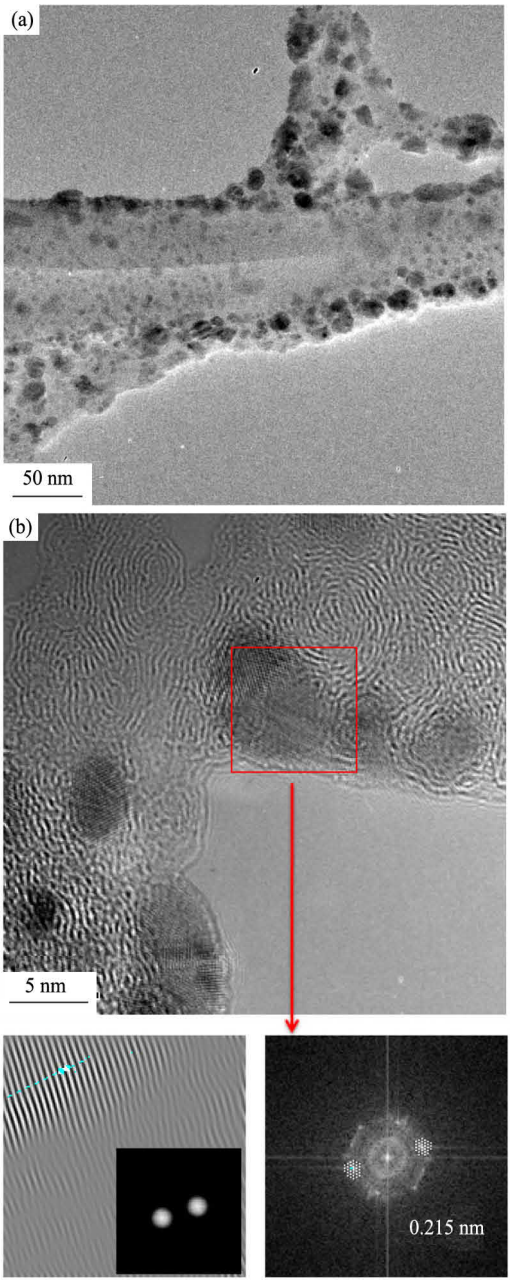

Fig. 5 High-resolution electron micrographs of $BaTiO_3:Yb^{3+}$ (6 mol.%) nanopowders obtained by hydrothermal method at 180° C and 36 h (a) and Fourier transform for (200) planes (b)

across a particle. If a particle is a single crystalline one, and has no strain, it should be uniform in contrast. However, if the TEM image shows dark-bright variation in contrast for a single crystalline particle, it is likely to have high strain within the grain.

In the lattice image of $BaTiO_3:Er^{3+}$ and $BaTiO_3:Yb^{3+}$, nanopowders were detected in planes (100), (110), and (200), with inter-planar distances of 0.404, 0.292 and 0.215 nm, respectively.

These planes correspond to the $BaTiO_3$ cubic phase, and this could be explained by the small size of the nanocrystals present, which are so small that the structural defects in the particles prevent the completion of the

structural transition, leading to high strain within the crystals[26]. The structural defects of nanocrystals occur primarily in the form of lattice OH^- ions, which are compensated for by barium vacancies (V''_{Ba}) created on the surfaces of individual particles to maintain electro-neutrality[39].

Since there is a high degree of strain inside the nanocrystals, some distortion of the cubic structure does occur, but it is obviously not sufficient to result in the formation of the tetragonal phase.

3 Conclusions

The crystalline powders of $BaTiO_3:Er^{3+}$ and $BaTiO_3:Yb^{3+}$ were synthesized successfully by the hydrothermal method. Using this procedure, it was possible to obtain materials that present a primarily cubic structure at low temperature (180 °C), which represents an advantage over other methods that require high temperatures to synthesize materials with the same phase. The results confirmed the presence of a stable cubic phase at room temperature, if the barium titanate particles were below 30 nm in size.

Acknowledgements: Garrido Hernández A acknowledges the M. Sc. scholarship from CONACYT. The authors would also like to thank David Nentwick for the editing work that he did for this paper. The authors would also like to thank M. García Murillo for her assistance.

References:

[1] Buscaglia M T, Buscaglia V, Viviani M, Nanni P. Atomistic simulation of dopant incorporation in barium titanate. *J. Am. Ceram. Soc.*, 2001, **84**: 376.

[2] Fu D S, Hao S E, Li J L, Qiang L S. Effects of the penetration temperature on structure and electrical conductivity of samarium modified $BaTiO_3$ powders. *J. Rare Earths*, 2011, **29**(2): 164.

[3] Tsur Y, Dunbar T D. Randall C A. Crystal and defect chemistry of rare earth cations in $BaTiO_3$. *J. Electroceramics*, 2001, **7**: 25.

[4] Pu Y P, Yang W H, Chen S T. Influence of rare earths on electric properties and microstructure of barium titanate ceramics. *J. Rare Earths*, 2007, 25(1): 154.

[5] Zhang Y, Hao J. Metal-ion doped luminescent thin films for optoelectronic applications. *J. Mater. Chem. C*, 2013, **1**: 5607.

[6] Zhang Y, Hao J, Mak C L, Wei X. Effects of site substitutions and concentration on upconversion luminescence of Er^{3+}-doped perovskite titanate. *Opt. Express*, 2011, **19**(3): 1824.

[7] Hao J, Zhang Y, Wei X. Electric-induced and modulation of upconversion photoluminescence in epitaxial $BaTiO_3$:Yb/Er thin films. *Angew. Chem. Int. Edit*., 2011, **50**: 6876.

[8] Zhang Y, Hao J. Color-tunable upconversion luminescence of Yb^{3+}, Er^{3+}, and Tm^{3+} tri-doped ferroelectric $BaTiO_3$ materials. *J. Appl. Phys.*, 2013, **113**(18): 184112-1, 184112-4.

[9] Viviania M, Lemaitreb J, Buscaglia M T. Low-temperature aqueous synthesis (LTAS) of $BaTiO_3$: a statistical design of experiment approach. *J. Eur. Ceram. Soc*., 2000, **20**(3): 315.

[10] Pinceloup P, Courtois C, Vicens J, Leriche A, Thierry B. Evidence of a dissolution-precipitation mechanism in hydrothermal synthesis of barium titanate powders. *J. Eur. Ceram. Soc*., 1999, **19**: 973.

[11] Guido B, Buscagalia V, Leoni M, Nanni P. Solid-state and surface spectroscopic characterization of $BaTiO_3$ fine powders. *Chem. Mater.*, 1994, **6**: 955.

[12] Durán P, Capel F, Gutierrez D, Tartaj J, Bañares M A, Mourea C. Metal citrate polymerized complex thermal decomposition leading to the synthesis of $BaTiO_3$: effects of the precursor structure on the $BaTiO_3$ formation mechanism. *J. Mater. Chem.*, 2001, **11**: 1828.

[13] Hwang U Y, Park H S, Koo K K. Low-temperature synthesis of fully crystallized spherical $BaTiO_3$; particles by the gel-sol method. *J. Am. Ceram. Soc*., 2004, **87**: 2168.

[14] Zhao X L, Ma Z M, Xiao Z J, Chen G. Preparation and characterization on nano-sized barium titanate powder doped with lanthanum by sol-gel process. *J. Rare Earths*, 2006, **24**(1): 82.

[15] Lee J H, Won C W, Kim, T S, Kim H S. Characteristics of $BaTiO_3$ powders synthesized by hydrothermal process. *J. Mater. Sci.*, 2000, **35**(17): 4271.

[16] Lee S K, Park T J, Choi G J, Koo K K, Sang W K. Effects of KOH/BaTi and Ba/Ti ratios on synthesis of $BaTiO_3$ powder by coprecipitation/hydrothermal reaction. *Mater. Chem. Phys.*, 2003, **82**: 742.

[17] Pinceloup P, Courtois C, Leriche A, Thierry B. Hydrothermal synthesis of nanometer-sized barium titanate powders: control of barium/titanium ratio, sintering, and dielectric properties. *J. Am. Ceram. Soc.*, 1999, **82**(11): 3049.

[18] Xu H R, Gao L, Guo J K. Preparation and characterizations of tetragonal barium titanate powders by hydrothermal method. *J. Eur. Ceram. Soc.*, 2002, **22**(7): 1163.

[19] García-Hernández M, Chadeyron G, Boyer D. García-Murillo A, Carrillo-Romo F, Mahiou R. Hydrothermal synthesis and characterization of europium-doped barium titanatenanocrystallites. *Nano-Micro Lett*., 2013, **5**(1): 57.

[20] Strek W, Hreniak D, Boulon G, Guyot Y, Pazik R. Optical behavior of Eu^{3+}-doped $BaTiO_3$ nano-crystallites prepared by sol-gel method. *Opt. Mater*, 2003, **24**(1-2): 15.

[21] Amami J, Hreniak D, Guyot Y, Pazik R, Goutaudier C, Boulon G, Ayadi M, Strek W. Second harmonic generation and Yb^{3+} cooperative emission used as structural probes in size-driven cubic-tetragonal phase transition in $BaTiO_3$ sol-gel nanocrystals. *J. Lumin.*, 2006, **119**: 383.

[22] Arlt G, Hennings D, de With G. Dielectric properties of fine-grained barium titanate ceramics. *J. Appl. Phys*., 1985, **58**: 1619.

[23] Asiaie R, Zhu W, Akbar S A, Dutta P K. Characterization of submicron particles of $BaTiO_3$. *Chem. Mater.*, 1996, **8**: 226.

[24] Busca G, Ramis G, Gallardo J M, Sanchez V, Piaggio P. FT Raman and FTIR studies of titanias and metatitanate powders. *J. Chem. Soc*., 1994, **90**: 3181.

[25] Yanfeng G, Yoshitake M, Zifei P, Tetsu Y, Kunihito K. Room temperature deposition of a TiO_2 thin film from aqueous peroxotitanate solution. *J. Mater. Chem.*, 2003, **13**: 608.

[26] Wada S, Chikamori H, Noma T, Suzuki T. Synthesis of nm-sized barium titanate crystallites using a new LTDS method and their characterization. *J. Mater. Sci.*, 2000, **35**(19): 4857.

[27] Hennings F K, Metzmacher C, Schreinemacher B S. Defect chemistry and microstructure of hydrothermal barium titanate. *J. Am. Ceram. Soc*., 2001, **84**(1): 179.

[28] Du Y L, Zhang M S, Chen Q, Yin Z. Investigation of size-driven phase transition in bismuth titanatenanocrystals by Raman spectroscopy. *Appl. Phys.*, 2003, **76**(7): 1099.

[29] Chandler C D, Roger C, Hampden-Smith M J. Chemical aspects of solution routes to perovskite-phase mixed-metal oxides from metal-organic precursors. *Chem. Rev.*, 1993, **93**(3): 1205.

[30] Iain J C, Tomanari T, Noikazu O, Derek C S. Hydrothermal synthesis and characterisation of $BaTiO_3$ fine powders: precursors, polymorphism and properties. *J. Mater. Chem.*, 1999, **9**: 83.

[31] Jiang B, Peng J L, Bursill L A, Ren T L, Zhang P L, Zhong W L. Defect structure and physical properties of barium titanate ultra-fine particles. *Physica B*, 2000, **291**(1–2): 203.

[32] Yang G, Yue Z X, Sun T Y, Zhao J Q, Li L T. Investigation of ferroelectric phase transition for modified barium titanate in multilayer ceramic capacitors by in situ Raman scattering and dielectric measurement. *Appl. Phys. A*, 2008, **91**(1): 119.

[33] Freya M H, Xua Z, Hana P, Paynea D A. The role of interfaces on an apparent grain size effect on the dielectric properties for ferroelectric barium titanate ceramics. *Ferroelectrics*, 1998, **206**: 337.

[34] Doba P S, Dixi A, Katiyar R S. Effect of lanthanum substitution on the Raman spectra of barium titanate thin films. *J. Raman. Spectrosc.*, 2007, **38**(2): 142.

[35] Cifti E, Rahaman M N, Shumsky M. Hydrothermal precipitation and characterization of nanocrystalline $BaTiO_3$ particles, *J. Mater. Sci*., 2001, **36**(20): 4875.

[36] Tan T. Ferrolectric Thin Films III, Symposium Proceedings. Lauser Eds. Materials Research Society, 1993. 269.

[37] Moon J, Li T, Randalla C A, Adair J H. Low temperature synthesis of lead titanate by a hydrothermal method. *J. Mater. Res.*, 1997, **12**(1): 189.

[38] Zhua X, Zhu J, Zhou S, Liu Z, Ming N, Hesse D. $BaTiO_3$ nanocrystals: Hydrothermal synthesis and structural characterization. *J. Cryst. Growth*, 2005, **283**(3-4): 553.

[39] Hennings D, Schreinemacher S. Characterization of hydrothermal barium titanate. *J. Eur. Ceram. Soc*., 1992, **9**: 41.